

## Resonance-enhanced dipolar interaction between terahertz photons and confined acoustic phonons in nanocrystals

Tzu-Ming Liu, Ja-Yu Lu, Hung-Ping Chen, Chung-Chiu Kuo, Meng-Ju Yang, Chih-Wei Lai, Pi-Tai Chou, Ming-Hao Chang, Hsiang-Lin Liu, Yu-Tai Li, Ci-Ling Pan, Shih-Hung Lin, Chieh-Hsiung Kuan, and Chi-Kuang Sun

Citation: *Applied Physics Letters* **92**, 093122 (2008); doi: 10.1063/1.2891062

View online: <http://dx.doi.org/10.1063/1.2891062>

View Table of Contents: <http://scitation.aip.org/content/aip/journal/apl/92/9?ver=pdfcov>

Published by the [AIP Publishing](#)

---

### Articles you may be interested in

**Effects of nanocrystal shape and size on the temperature sensitivity in Raman thermometry**  
*Appl. Phys. Lett.* **103**, 083107 (2013); 10.1063/1.4819170

**Acoustic phonon strain induced mixing of the fine structure levels in colloidal CdSe quantum dots observed by a polarization grating technique**  
*J. Chem. Phys.* **132**, 104506 (2010); 10.1063/1.3350871

**Enhanced two-photon absorption of CdS nanocrystal rods**  
*Appl. Phys. Lett.* **94**, 103117 (2009); 10.1063/1.3100196

**Optical and dielectric properties of ZnO tetrapod structures at terahertz frequencies**  
*Appl. Phys. Lett.* **89**, 031107 (2006); 10.1063/1.2222329

**Confined optical modes in small photonic molecules with semiconductor nanocrystals**  
*J. Appl. Phys.* **96**, 6761 (2004); 10.1063/1.1812355

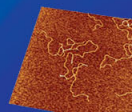
---

### NEW! Asylum Research MFP-3D Infinity™ AFM

Unmatched Performance, Versatility and Support



Stunning high performance



Simpler than ever to GetStarted™

Comprehensive tools for nanomechanics



Widest range of accessories for materials science and bioscience



# Resonance-enhanced dipolar interaction between terahertz photons and confined acoustic phonons in nanocrystals

Tzu-Ming Liu,<sup>1</sup> Ja-Yu Lu,<sup>1</sup> Hung-Ping Chen,<sup>1</sup> Chung-Chiu Kuo,<sup>1</sup> Meng-Ju Yang,<sup>2</sup> Chih-Wei Lai,<sup>2</sup> Pi-Tai Chou,<sup>2</sup> Ming-Hao Chang,<sup>3</sup> Hsiang-Lin Liu,<sup>3</sup> Yu-Tai Li,<sup>4</sup> Ci-Ling Pan,<sup>4</sup> Shih-Hung Lin,<sup>5</sup> Chieh-Hsiung Kuan,<sup>5</sup> and Chi-Kuang Sun<sup>1,5,6,a)</sup>

<sup>1</sup>Graduate Institute of Photonics and Optoelectronics, National Taiwan University, Taipei 10617, Taiwan, Republic of China

<sup>2</sup>Department of Chemistry, National Taiwan University, Taipei 10617, Taiwan, Republic of China

<sup>3</sup>Department of Physics, National Taiwan Normal University, Taipei 11650, Taiwan, Republic of China

<sup>4</sup>Department of Photonics, National Chiao Tung University, Hsinchu 300, Taiwan, Republic of China

<sup>5</sup>Department of Electrical Engineering, National Taiwan University, Taipei 10617, Taiwan, Republic of China

<sup>6</sup>Research Center for Applied Sciences, Academia Sinica, Taipei 10617, Taiwan, Republic of China

(Received 29 October 2007; accepted 1 February 2008; published online 6 March 2008; publisher error corrected 13 March 2008)

Taking advantage of the specific core-shell charge separation structure in the CdSe/CdTe core-shell type-II nanocrystals, we experimentally observed and verified the existence of the resonance-enhanced dipolar interaction between terahertz photons and their corresponding confined acoustic phonons. From the measured terahertz transmission spectra, we found that the photon frequency of the terahertz resonant absorption is inversely proportional to the diameter  $D$  of the nanocrystals and agrees with that of dipolar active  $l=1, n=0$  confined acoustic modes. The corresponding absorption cross section shows a  $D^4$  dependence, supporting a charged simple-harmonic-oscillator model. These facts verify the occurrence of dipolar interaction between terahertz photons and confined terahertz acoustic phonons. © 2008 American Institute of Physics. [DOI: 10.1063/1.2891062]

With spatial confinement, low dimensional systems such as quantum dots and nanowires exhibit not only electronic but also acoustic energy quantization. In 1882, Lamb had already studied the acoustic normal modes confined in a homogeneous free sphere.<sup>1</sup> Two types of modes, torsional and spheroidal (SPH), were derived from the stress-free boundary condition on the spherical surface. According to the selection rule,<sup>2</sup> among these modes, only SPH modes with angular momentum quantum number  $l=1$  can induce terahertz absorption, which was not experimentally observed until a recent report on terahertz absorption in  $\text{TiO}_2$  nanopowders.<sup>3</sup> The authors proposed that it could result from dipolar interaction with the SPH:  $l=1$  confined acoustic modes. As for the required charge separation for activating terahertz absorption, they suspected that it could come from the unintentionally adsorbed water molecules.<sup>3</sup> It is thus highly desirable to create specific spatial charge separation in nanoparticles as a template to verify the existence of the SPH:  $l=1$  related terahertz absorption, which was theoretically predicted so long ago. This is not only important for the studies of nanoacoustics but could also be critical for future development of terahertz technologies.

In this letter, we exploited the well-known core-shell charge separation in CdSe/CdTe core-shell type-II nanocrystals<sup>4</sup> (NCs) to directly prove the existence of the resonance-enhanced dipolar interaction between terahertz photons and the fundamental  $l=1$  confined acoustic phonons

in NCs. Our study also reveals the fact that the cross section of the dipolar terahertz absorption,  $\sigma_{\text{ex}}$ , varies with a fourth power dependence on the particle size  $D$ , agreeing well with a prediction based on an electromechanical model.<sup>3</sup>

The SPH vibrations in a free homogeneous isotropic continuum sphere can modify its optical properties<sup>2</sup> and induce either inelastic light scattering<sup>5,6</sup> or terahertz absorption.<sup>3</sup> The former processes are related to the SPH modes with  $l=0$  or 2, which have been widely investigated through low-frequency Raman scattering,<sup>5</sup> Brillouin scattering,<sup>6</sup> and pulsed laser pump-probe experiments.<sup>7</sup> In contrast, the latter process is related only to the scarcely studied  $l=1$  mode.<sup>3</sup> Distributions of the displacement vector of the  $l=1$  modes show relative displacement between the center core and the outer shell regions.<sup>3</sup> Therefore, a core-shell charge separation is required to match this motional pattern, to induce change of dipole moment, and to activate the resonant absorption of the SPH:  $l=1$  dipolar mode. However, it is hard for inorganic clusters to create specific and long term charge separation. Besides, the amount of charge should be large enough to induce detectable excess absorption over the background dielectric absorption.<sup>8</sup> Following these requirements, we prepared CdSe/CdTe core/shell type-II NCs by chemical synthesis.<sup>9</sup> Due to a large surface to volume ratio, the surface lone pairs on the tellurium dangling bonds<sup>10</sup> could be thermally or optically excited to the conduction band of CdTe and fall into the CdSe core with lower electronic potential. This process can result in a negatively charged core and a positively charged ion shell on the CdTe surface. This specific core-shell charge separation should en-

<sup>a)</sup>Author to whom correspondence should be addressed. Electronic mail: sun@cc.ee.ntu.edu.tw.

able the studies of the dipolar interaction between terahertz photons and confined acoustic modes in NCs.

The synthesis of CdSe/CdTe NCs followed the steps described previously.<sup>9</sup> We synthesized  $3.6 \times 10^{15}$ ,  $1.4 \times 10^{16}$ , and  $1.6 \times 10^{16}$  particles in the powder form of 8 nm (4.3 nm core), 10.4 nm (4.3 nm core), and 13 nm (5.3 nm core) CdSe/CdTe type-II NCs. From transmission electron microscope images, it was determined that the size standard deviation was  $\sim \pm 20\%$ . Their absorption spectra smoothly extended to red and near infrared without a steep absorption edge. Their emission spectrum peaks around 1100 nm. The infrared sample emission indicates recombination between CdSe electrons and CdTe holes, which validates the presence of type-II band alignment in our samples. These NC powders were separately sealed between two 30- $\mu\text{m}$ -thick polyethylene films for the convenience of holding in the terahertz measurements.

The experimental setup for the terahertz absorption spectroscopy was similar to that in a previous work.<sup>11</sup> We employed a photonic transmitter to generate terahertz pulses with a tunable central frequency. The spectral power of coherence-controlled terahertz source reached a maximum at 100 GHz and extended to 400 GHz with a substantial signal to noise ratio. The radiated terahertz wave was collected by two parabolic reflectors and focused on a bolometer. The NC sample was put in front of the bolometer for the measurement. Dividing the transmission spectra with NCs by that without NCs, the spectra of transmission  $T$  can be obtained. To evaluate the absorption contributed from each NC, we derived the extinction cross section  $\sigma_{\text{ex}}$  for excess terahertz absorption of each NC by  $\sigma_{\text{ex}} = \ln(T)A/N$ , where  $A$  is the excitation area and  $N$  is the number of NCs in the excitation area. For 13 nm NCs, the  $\sigma_{\text{ex}}$  spectrum shows  $165 \pm 40$  and  $370 \pm 60$  GHz peaks with a 250 GHz shoulder [Fig. 1(a)]. We then measured two  $\sigma_{\text{ex}}$  peaks of  $200 \pm 40$  and  $360 \pm 70$  GHz [Fig. 1(b)] for 10.4 nm NCs and two  $\sigma_{\text{ex}}$  peaks of  $210 \pm 31$  and  $380 \pm 50$  GHz [Fig. 1(c)] for 8 nm NCs. To study the second and the third spectral peaks with a higher spectral resolution and better signal to noise ratio, we double-checked the terahertz absorption with a time domain spectroscopy (TDS) system.<sup>12</sup> Its power spectrum ranged between 0.1 and 0.7 THz with a 10 GHz resolution. For the terahertz TDS measurement, we prepared 8.4, 10.1, and 11.6 nm CdSe/CdTe NC samples. All samples show strong dielectric absorption for frequencies higher than 400 GHz, making the corresponding transmission signal well below the noise level. Figure 1(d) shows the trace of the 11.6 nm sample within 100–400 GHz spectral range. The  $\sigma_{\text{ex}}$  spectrum shows clear first absorption peaks at  $170 \pm 17$  GHz and two satellite peaks at  $271 \pm 15$  and  $333 \pm 15$  GHz. For the 10.1 nm sample, the  $\sigma_{\text{ex}}$  spectrum shows a  $175 \pm 34$  GHz peak and an oscillating second peak around 322 GHz [Fig. 1(e)]. For the 8.4 nm sample, there is only a  $170 \pm 17$  GHz peak [Fig. 1(f)].

To check the measured resonant frequencies against theory, we calculated the eigenfrequency  $\nu$  of the SPH: $l=1$  modes by the eigenvalue equation with  $l=1$  (Ref. 6),

$$4 \frac{j_2(\xi)}{j_1(\xi)} \xi - \eta^2 + 2 \frac{j_2(\eta)}{j_1(\eta)} \eta = 0, \quad (1)$$

where  $\xi = \pi \nu D / V_L$ ,  $\eta = \pi \nu D / V_T$ , and  $j_1(\eta)$  is the spherical Bessel function of the first kind;  $V_L$  and  $V_T$  are the sound

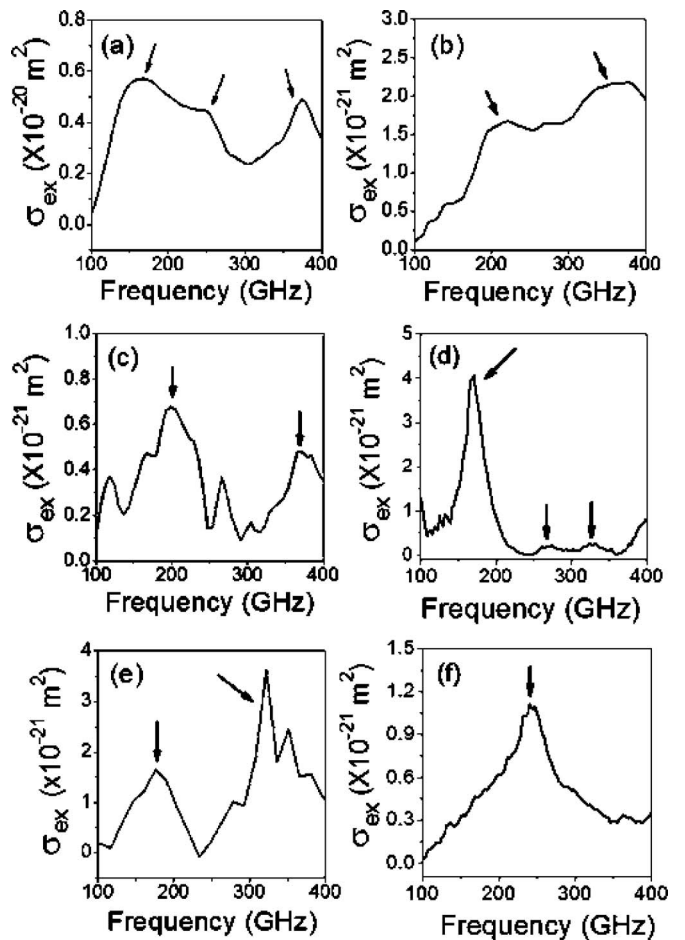


FIG. 1. The spectra of the extinction cross section  $\sigma_{\text{ex}}$  of (a) 13, (b) 10.4, (c) 8, (d) 11.6, (e) 10.1, and (f) 8.4 nm CdSe/CdTe NCs. The black arrows indicate the position of extinction peaks.

velocities of longitudinal and transverse waves, respectively. Because the acoustic properties of CdSe ( $V_L=3570$  m/s,  $V_T=1720$  m/s) (Ref. 13) and CdTe ( $V_L=3411$  m/s,  $V_T=1756$  m/s) (Ref. 14) are very similar, we treated the NCs acoustically as CdSe spheres. Using the acoustic parameters of CdSe, the calculated frequency of the SPH: $l=1:n=0$  mode for 10.4 nm CdSe/CdTe NCs is 191 GHz, where  $n$  is the mode index. Considering the resolution of our source and the uncertainties in the size distribution, the frequency of our measured first extinction peak in 10.4 nm case agrees with theoretical prediction. At the frequency of peak absorption, the transmitted terahertz power decayed to 0.65 of the original, corresponding to  $\sim 2 \times 10^{-21} \text{ m}^2$  of  $\sigma_{\text{ex}}$ . Extrapolated from the Fourier transform infrared spectroscopy measurement, the corresponding dielectric absorption cross section of 10.4 nm NCs is in the order of  $2 \times 10^{-22} \text{ m}^2$  around the fundamental resonant frequency of the SPH: $l=1$  modes. It is much less than the measured value of the 10.4 nm NCs.

For other samples, considering size variation and absorption bandwidth, the measured frequencies of the first peaks [Fig. 2(a), solid squares] also agree well with the calculated resonant frequencies of the SPH: $l=1:n=0$  phonons [Fig. 2(a), solid line] with an inverse dependence on the particle size  $D$ . For the measured frequencies of the second and third absorption peaks [see Fig. 2(a), open circles], some of them match SPH: $l=1:n=1$  phonons [Fig. 2(a), dotted line] and some of them match the SPH: $l=0:n=0$  phonons [Fig. 2(a),

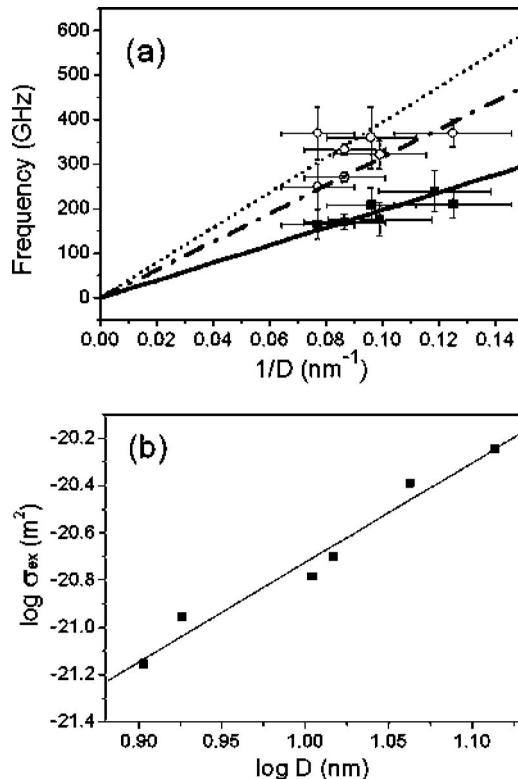


FIG. 2. (a) Frequencies of  $\text{SPH}:l=1:n=0$  phonons (solid line),  $\text{SPH}:l=1:n=1$  phonons (dotted line),  $\text{SPH}:l=0:n=0$  phonons (dash-dotted line), and the terahertz absorption peaks (solid squares for first absorption peaks and open circles for other peaks) as a function of inverse NC size  $1/D$ . The error bars express the size variation and the terahertz absorption bandwidth. (b) Extinction cross section of excess terahertz absorption corresponding to the  $\text{SPH}:l=1:n=0$  phonons as a function of particle diameter  $D$ . The fitting line (solid curve) has a slope of 4.2.

dash-dotted line]. The appearance of  $\text{SPH}:l=0:n=0$  modes related absorption could be due to the shape-asymmetry induced nonuniform charge distribution of the NCs. The disappearance of  $\text{SPH}:l=1:n=1$  modes could be due to the reduced  $\sigma_{\text{ex}}$  for small particle size, the rise of dielectric background absorption at higher frequency, or contributed from the relatively lower signal level after 400 GHz. The source of the deviation from theoretical prediction could probably result from the aggregation induced interparticle interaction or from the fact that the shape of the NCs is not an ideal sphere. Removing the contribution from dielectric absorption, the peak  $\sigma_{\text{ex}}$  for the  $\text{SPH}:l=1:n=0$  modes of 13, 11.6, 10.1, 8.4, and 8 nm samples are  $5.7 \times 10^{-21}$ ,  $4.1 \times 10^{-21}$ ,  $1.6 \times 10^{-21}$ ,  $1.1 \times 10^{-21}$ , and  $7 \times 10^{-22} \text{ m}^2$ , respectively. Together with the  $\sigma_{\text{ex}}$  of 10.4 nm NCs, it is worth noting that

these data can be fitted by the equation  $\sigma_{\text{ex}} = aD^4$  [Fig. 2(b), solid curve]. According to the electromechanical model of Murray *et al.*,  $\sigma_{\text{ex}}$  of the  $\text{SPH}:l=1$  modes is proportional to  $Q^2$ .<sup>3</sup> Combining it with our results gives  $Q \propto D^2$ , indicating that the amount of spatial separated charges is proportional to the surface area of the NCs. This conclusion is consistent with our proposal that separated charges come from the surface defect (tellurium dangling bonds) related donors.

In conclusion, we synthesized CdSe/CdTe type-II NCs for the investigation and verification of terahertz absorption related to the  $\text{SPH}:l=1:n=0$  mode. The specific core-shell charge separation, which is the key to activate the terahertz resonant absorption, was achieved by the surface defect related donors and the type-II alignment. From the terahertz absorption spectra, the first resonant frequency shows a  $1/D$  dependence and agrees with that of  $\text{SPH}:l=1:n=0$  mode predicted by the elastic continuum theory. Our results directly prove the existence of resonance-enhanced dipolar interaction between terahertz photons and  $\text{SPH}:l=1$  confined acoustic phonons in NCs.

This project is sponsored by the National Science Council of Taiwan under Grant Nos. NSC96-2120-M-002-014 and NSC 96-2628-E-002-043-MY3 and by the National Taiwan University Research Center for Medical Excellence. We thank D. B. Murray and L. Saviot for technical discussions on the dipolar modes in a nanosphere.

<sup>1</sup>H. Lamb, *Proc. London Math. Soc.* **13**, 189 (1882).

<sup>2</sup>E. Duval, *Phys. Rev. B* **46**, 5795 (1992).

<sup>3</sup>D. B. Murray, C. H. Netting, L. Saviot, C. Pighini, N. Millot, D. Aymes, and H.-L. Liu, *J. Nanoelectron. Optoelectron.* **1**, 92 (2006).

<sup>4</sup>S. Kim, B. Fisher, H.-J. Eisler, and M. Bawendi, *J. Am. Chem. Soc.* **125**, 11466 (2003).

<sup>5</sup>E. Duval, A. Boukenter, and B. Champagnon, *Phys. Rev. Lett.* **56**, 2052 (1986).

<sup>6</sup>M. H. Kuok, H. S. Lim, S. C. Ng, N. N. Liu, and Z. K. Wang, *Phys. Rev. Lett.* **90**, 255502 (2003).

<sup>7</sup>T. D. Krauss and F. W. Wise, *Phys. Rev. Lett.* **79**, 5102 (1997).

<sup>8</sup>S.-I. Lee, T. W. Noh, K. Cummings, and J. R. Gaines, *Phys. Rev. Lett.* **55**, 1626 (1985).

<sup>9</sup>C.-Y. Chen, C.-T. Cheng, C.-W. Lai, Y.-H. Hu, P.-T. Chou, Y.-H. Chou, and H.-T. Chiu, *Small* **1**, 1215 (2005).

<sup>10</sup>S. K. Poznyak, N. P. Osipovich, A. Shavel, D. V. Talapin, M. Gao, A. Eychmüller, and N. Gaponik, *J. Phys. Chem. B* **109**, 1094 (2005).

<sup>11</sup>J.-Y. Lu, L.-J. Chen, T.-F. Kao, H.-H. Chang, H.-W. Chen, A.-S. Liu, Y.-C. Chen, R.-B. Wu, W.-S. Liu, J.-I. Chyi, and C.-K. Sun, *IEEE Photonics Technol. Lett.* **18**, 2254 (2006).

<sup>12</sup>C.-L. Pan, C.-F. Hsieh, R.-P. Pan, M. Tanaka, F. Miyamaru, M. Tani, and M. Hangyo, *Opt. Express* **13**, 3921 (2005).

<sup>13</sup>D. L. Rode, *Phys. Rev. B* **2**, 4036 (1970).

<sup>14</sup>E. Deligoz, K. Colakoglu, and Y. Ciftci, *Physica B* **373**, 124 (2006).